Proceedings of the

1996 IEEE/RSJ International Conference on Intelligent Robots and Systems

IROS 96

Robotic Intelligence Interacting with Dynamic Worlds

November 4-8, 1996

Senri Life Science Center, Osaka, Japan

Volume 2

Sponsored by
IEEE Industrial Electronics Society
IEEE Robotics and Automation Society
Robotics Society of Japan
Society of Instrument and Control Engineers
New Technology Foundation

Vision Based Active Antenna
— Basic Considerations on Two-Points Detecting Method —

Naoki Kanayama Makoto Kaneko Toshio Tsuji

Industrial and Systems Engineering
Hiroshima University
Kagamiyama Higashi-Hiroshima 739, Japan

Abstract

This paper is an extended version of the Vision Based Active Antenna (VBAA) that can detect the contact force, the stiffness of the environment, and the contact location between an insensitive elastic antenna and an environment, through the observation of the antenna's shape by a camera [8]. If measured points are on the antenna, two arbitrary points are sufficient for computing the contact location and the contact force uniquely. In a practical application of VBAA, however, the measured points are not always on the antenna. In this paper, we show the condition for uniquely obtaining both contact location and contact force under the situation that the measured points are not always on the antenna. We also show a new compensation method to improve the sensing accuracy. We further verify our idea experimentally.

1 Introduction

The Vision Based Active Antenna (VBAA) is a new sensing system enabling us to detect the contact location between an insensitive elastic antenna and an environment, the contact force, and the stiffness of the environment through observation of the antenna's shape. The VBAA is simply composed of one insensitive elastic antenna, one actuator to rotate the antenna, one position sensor to measure the rotation angle of the antenna, and one CCD camera to observe the antenna's shape, as shown in Fig.1.

A simple flexible beam sensor can take the form of a short length of spring piano wire or hypodermic tubing anchored at the end. When the free end touches an external object, the wire bends. This can be sensed by a piezoelectric element or by a simple switch [9]. A more elaborate sensor is described by Wang and Will [10]. Long antennae-like whisker sensors were mounted on the SRI mobile robot, Shakey [11], and on Rodney Brook's six-legged robot insects [12]. Hirose, et.al. discussed the utilization of whisker sensors in legged robots [13]. Similarly shaped whiskers have been considered for the legs of the Ohio State University active suspension vehicle [14]. The major difference between previous works [9]–[14] and ours is that the VBAA can detect not only the contact point between the antenna and the environment but also the environment's stiffness, while previous works do not.

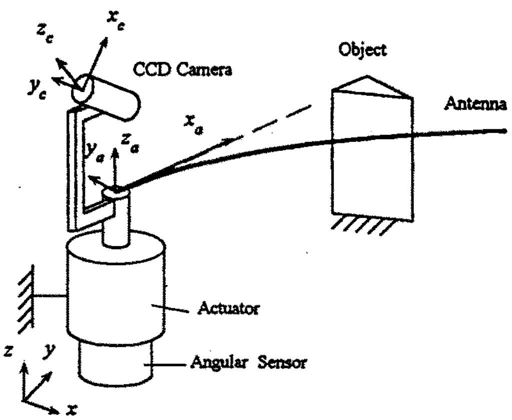

Figure 1: An overview of VBAA.

There are several works combining both tactile and vision sensors to take advantage of each sensor. For example, Stansfield presented a robotic perceptual system which utilizes passive vision and active touch [15]. Allen proposed an object recognition system that uses passive stereo vision and active exploratory tactile sensing [16]. These works utilized two different kinds of sensors to increase sensing ability. In the VBAA, a vision sensor is utilized for indirectly evaluating the contact force and the contact point.

In our former work, we have shown that if the environment is rigid, the contact location is a function of the rotational compliance of the antenna in contact with the environment, and that it can be obtained by utilizing the outputs from both joint position and torque sensors. Such a sensing system has been termed the Active Antenna [1, 2, 3]. This idea has also been extended to a 3D version [4, 5]. Ueno and Kaneko discussed the Dynamic Active Antenna, in which the contact location is estimated through the measurement of natural frequency of a flexible beam whose dynamics is changed according to the contact location between the environment and itself [6, 7]. A big advantage of the Active Antenna is that a location of the contact point is obtained through a surprisingly simple active motion, while sophisticated active motions should be prepared in most contact sensing methods in order to

Proc. IROS 96
0-7803-3213-X/96/ $ 5.00

avoid large interaction force between the sensor and the environment. This is because the flexibility of the antenna itself successfully relaxes the contact force, even under a large positional error.

However, the Active Antenna cannot work appropriately in a compliant environment, since the sensor system is not able to break down the measured compliance into that coming from the antenna itself and that coming from the environment. The difficulty of decomposition comes from the sensor system utilizing only local information, such as the joint torque and the joint angular displacement, but not taking any global information into consideration. This is the reason why a vision system is introduced into the VBAA. An active motion is imparted to the antenna for environment sensing. The camera continuously observes the antenna's shape. By observing the shape distortion from it's original straight line position, the sensor system can detect any initial contact with the environment. With further active motion, the antenna deforms according to the pushing angle, the contact location, and the environment's stiffness. The pushing angle can be regarded as input for the VBAA, and the antenna's shape obtained through the CCD camera can be regarded as the output. By analyzing proceeding the input-output relationship, the VBAA can detect the contact distance, the contact force, and the environment's stiffness. We would emphasize that the vision in the VBAA is not used to detect the contact point directly but used to observe the antenna's shape. Because of this feature, the VBAA can detect both contact location and contact force even though the exact contact point is hidden by occlusion. In order to measure stiffness, a position sensor and a force sensor are generally necessary in addition to the actuator which imparts the active motion. It can be understood that in the VBAA, a force is equally detectable through the observation of the elastic deformation of the antenna by a camera. Without elasticity of the antenna, it is impossible to evaluate both the contact force and the environment's stiffness, and so such elasticity of the antenna is quite essential to the VBAA.

We have already shown the basic working principle of the VBAA [8], in which a fitting method was conveniently used to estimate the antenna shape from the measured points. The fitting method works effectively but it takes a long time for computing and determining the antenna shape completely. Therefore, it is not appropriate for applying the method to a real time system. In this paper, we focus on the Two-Points Detecting Method. We have shown that two points are sufficient for uniquely determining the contact location and contact force, if they are exactly on the antenna [8]. Due to the digitizing error etc., however, it is extremely difficult to obtain the exact point on the antenna. As a result, the reconstructed antenna shape may not coincide with the original one.

In this paper, we first consider the condition for uniquely obtaining both the contact location and the contact force, even under that the measured points include the digitizing error. When two measured points cannot satisfy the condition, we can simply remove these two points and choose another combination of the measured points for computing both the contact location and the contact force. Each combination may provide different set of contact location and contact force. By applying averaging technique, we estimate both the contact location and the contact force. One big advantage is that the processing time based on the two-points detecting method is much shorter than that of the fitting method [8]. On the other hand, a disadvantage is that the two-points detecting method does not provide sufficiently good accuracy compared with the fitting method. In order to take advantage of the two-points detecting method, we propose a new compensation method by taking the pushing angle into consideration.

2 Structure of VBAA and Assumptions

2.1 Basic Structure of VBAA

Figure 1 shows basic structure of the VBAA. VBAA has insensitive flexible beam as antenna, one-axis motor for sensing motion, one-axis angular sensor and CCD camera for observing antenna's shape. Antenna is fixed on the rotation center of the motor.

We regard Σ_O as the world coordinate system, and Σ_a as the antenna coordinate. The antenna coordinate x_a is chosen so that the direction may coincide with the initial shape of the antenna. The antenna can rotate around z_a axis, and its rotation angle θ can be measured by using the angular sensor. The CCD camera of VBAA in Fig. 1 observes the antenna, the object and the background coming from the environment. We extract only antenna shape from digitized picture. This can be done more easily by using an artificially colored antenna. Since we can easily transform from the camera coordinate system to the antenna coordinate system, for simplify, we describe basic equations in the antenna coordinate system.

2.2 Main Assumptions

Main assumptions taken here are as follows:

Assumption 1: The antenna's motion is limited to a plane.

Assumption 2: The deformation of the antenna is small enough to ensure that the antenna's behavior obeys the force-deformation relationship obtained by linear theory.

Assumption 3: The environment (or the object) to be sensed is stationary during the active motions.

Assumption 4: All pixels concerning the antenna are already extracted from the scene.

3 Two-Points Detecting Method

3.1 Basic Equations of VBAA

Figure 2 shows the deformation of the antenna when force f is applied at the contact point l. In this case, the antenna shape is written as follows:

Curved Part $(0 < x_a \leq l \leq L)$,

$$y_a = \frac{f}{6EI}(3l - x_a)x_a^2 . \quad (1)$$

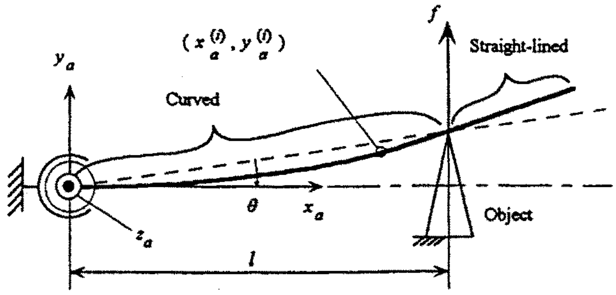

Figure 2: Top view of the VBAA.

Straight-Lined Part ($0 < l \le x_a \le L$),

$$y_a = \frac{f}{6EI}(3x_a - l)l^2, \tag{2}$$

where (x_a, y_a), l and L denote a point on the antenna coordinate system, the contact distance, and the total length of the antenna. In eqs. (1),(2), unknown parameters are f and l. So, the antenna shape is uniquely determined if f and l are given.

3.2 Uniqueness of Solution without Error [8]

Let us, first, discuss the ideal case in which the measured points are exactly on the antenna. Although the basic equations (1) and (2) are nonlinear with respect to l, we can easily solve for both l and f. The solution are given in the following.

(i) Two points from the curved part

From eq.(1), we can obtain the following two equations.

$$y_1 = \frac{f}{6EI}(3l - x_1)x_1^2, \tag{3}$$

$$y_2 = \frac{f}{6EI}(3l - x_2)x_2^2, \tag{4}$$

where l should satisfy the condition of $0 < x_1 < x_2 \le l$. From eq.(3) and (4), we can easily show the unique set of solutions in $0 < x_1 < x_2 \le l$ as follows,

$$\begin{cases} f = 6EI\dfrac{x_2^2 y_1 - x_1^2 y_2}{x_1^2 x_2^2 (x_2 - x_1)}, \\ l = \dfrac{x_1^3 y_2 - x_2^3 y_1}{3(x_1^2 y_2 - x_2^2 y_1)}. \end{cases} \tag{5}$$

Note that $x_2 - x_1 \ne 0$, $x_1^2 y_2 - x_2^2 y_1 \ne 0$, $x_1 \ne 0$, $x_2 \ne 0$ under $0 < x_1 < x_2 \le l$.

(ii) Two points from the straight-lined part

In this case, we can obtain the following two equations.

$$y_1 = \frac{f}{6EI}(3x_1 - l)l^2, \tag{6}$$

$$y_2 = \frac{f}{6EI}(3x_2 - l)l^2, \tag{7}$$

where l should satisfy the condition of $0 < l \le x_1 < x_2$. From eq.(6) and (7), we can introduce the unique set of solutions in $0 < l \le x_1 < x_2$ as follows,

$$\begin{cases} f = 2EI\dfrac{-(y_1 - y_2)^3}{9(x_2 - x_1)(x_1 y_2 - x_2 y_1)}, \\ l = \dfrac{3(x_1 y_2 - x_2 y_1)}{y_2 - y_1}. \end{cases} \tag{8}$$

Note that $x_2 - x_1 \ne 0$, $y_2 - y_1 \ne 0$, $x_1 y_2 - x_2 y_1 \ne 0$ under $0 < l \le x_1 < x_2$.

(iii) Points from each of the curved and straight-lined parts

Without lost of generality, we can assume $0 < x_1 \le l \le x_2$ and $x_1 \ne x_2$. In this case, eq.(3) and (7) exist. From these equations, we obtain,

$$g(l) = y_1 l^3 - 3x_2 y_1 l^2 + 3x_1^2 y_2 l - x_1^3 y_2 = 0. \tag{9}$$

Equation (9) is the third order equation with respect to l. From eq.(9), we can easily show eqs.(10) and (11) under $0 < x_1 \le l \le x_2$, $x_1 \ne x_2$ and $0 < f$.

$$\lim_{l \to -\infty} g(l) = -\infty \tag{10}$$

$$\lim_{l \to +\infty} g(l) = +\infty \tag{11}$$

Now, let us examine the sign of $g(x_1)$ and $g(x_2)$. $g(x_1)$ and $g(x_2)$ can be rearranged in the following forms.

$$\begin{aligned} g(x_1) &= \frac{f}{6EI}(l - x_1)x_1^3\{(3x_2 - x_1)(l - x_1) \\ &\quad + l(x_2 - x_1) + 2l(x_2 - l)\} \end{aligned} \tag{12}$$

$$\begin{aligned} g(x_2) &= -\frac{f}{6EI}x_1^2(x_2 - l)\{l(2x_2 + l)(x_2 - x_1) \\ &\quad + 2lx_2(x_2 - l) + 2x_2^2(l - x_1)\} \end{aligned} \tag{13}$$

Under the condition of $0 < x_1 \le l \le x_2$, $x_1 \ne x_2$ and $0 < f$, we can easily show $g(x_1) \ge 0$ and $g(x_2) \le 0$. Conditions (10), (11), $g(x_1) \ge 0$ and $g(x_2) \le 0$ ensures that we always have one real root between x_1 and x_2, while there are three real roots (double roots can be allowed) over the whole range.

Note that we cannot know beforehand whether measured point is on the curved or on the straight-lined part. A natural question that comes up is which solution should we use to compute the contact distance and the contact force. We can easily show that if we obtain unique set of solutions by using one of three cases, two other solutions never exist within the permissible region of solutions. This is summarized in Table 1, where "C" and "S" denote Curved and Straight-Lined, respectively. For example, when two points are both obtained from the curved part, only eq.(5) can satisfy the condition of solution ($0 < x_1 < x_2 \le l$), while eq.(8) and solution of eq.(9) cannot. Thus, we can always obtain the unique set of solution, if it is guaranteed that two points are exactly on the antenna. However, if this is not the case, the existence of solution may not be guaranteed. In the following sub-section, we discuss this matter in detail.

Table 1: Solution map.

	Eq.(5)	Solution of Eq.(9)	Eq.(8)
C, C	○	×	×
C, S	×	○	×
S, S	×	×	○

3.3 Uniqueness of Solution with Error

[Theorem] Let (x_1, y_1) and (x_2, y_2) be the observed points, where $0 < x_1 < x_2$, $0 < y_1$ and $0 < y_2$. The condition leading to the unique shape of the antenna is given by the following inequality.

$$\frac{y_2(3L - x_1)x_1^2}{(3L - x_2)x_2^2} \le y_1 \le \frac{y_2}{x_2}x_1 \qquad (14)$$

Proof: Let us consider the antenna shape always passing through the point (x_2, y_2) as shown in Fig. 3. Since it is be difficult to consider the condition of uniqueness of antenna shape under the condition that two points are fully arbitrary, we fix one point (x_2, y_2) and discuss the relative relationship to be satisfied between (x_1, y_1) and (x_2, y_2).
(i) Straight-lined part passes at point (x_2, y_2) is given by:

$$y_{sc} = \frac{y_2(3l - x_a)x_a^2}{(3x_2 - l)l^2} \quad (0 \le x_a \le l \le x_2), \qquad (15)$$

$$y_{ss} = \frac{y_2(3x_a - l)}{3x_2 - l} \quad (0 < l \le x_a \le x_2). \qquad (16)$$

We call eqs. (15) and (16) Antenna Shape Function. By partially differentiating eq. (15) and (16) with respect to l, we can obtain the following equations:

$$\frac{\partial}{\partial l}y_{sc} = \frac{3y_2x_a^2}{(3x_2 - l)^2l^3}\{(2l - x_a)(l - x_2) + (x_a - l)x_2\} < 0, \qquad (17)$$

$$\frac{\partial}{\partial l}y_{ss} = \frac{3y_2(x_a - x_2)}{(3x_2 - l)^2} < 0. \qquad (18)$$

Note that $\partial y_{sc}/\partial l$ and $\partial y_{ss}/\partial l$ are always negative in the range of $0 \le x_a \le l \le x_2$ and $0 < l \le x_a \le x_2$, respectively. This means that each Antenna Shape Function monotonically decreases with respect to l. Now, let us consider two antenna shapes (Fig. 4) whose contact distances are l_1 and l_2, respectively, where $0 < l_1 < l_2 \le x_2$. Since points A_1 and B_1 are both on the curved part, inequality $y_{A1} > y_{B1}$ is obvious as shown in Fig. 4 (monotony of y_{sc}). Similarly, since points A_2 and B_2 are on the straight-lined part, $y_{A2} > y_{B2}$ (monotony of y_{ss}). The segment A_1A_2 is straight-line, while the segment B_1B_2 is curved. Since the segment B_1B_2 is the lower convex curve, a point in the straight-line segment A_1A_2 always is upper than a point in the segment B_1B_2. Thus, we can say that

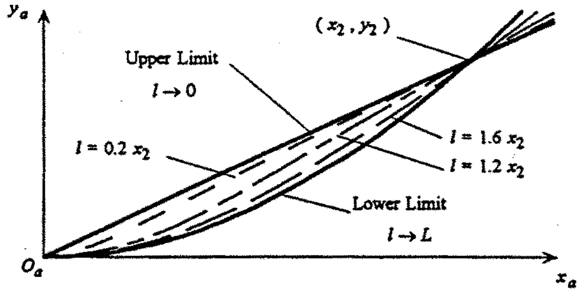

Figure 3: Upper and lower limit of Antenna shape depending on l.

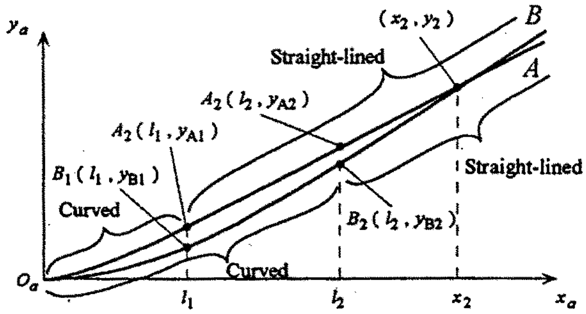

Figure 4: Antenna shapes decided by contact distance l_1 and l_2.

the Antenna Shape Function monotonically decreases over $0 \le x_a \le x_2$ with respect to l. Now, let us consider the upper and the lower limits of the Antenna Shape Function. By taking $l \to 0$, the upper limit is given by

$$\lim_{l \to 0} y_{ss} = \frac{y_2}{x_2}x_a. \qquad (19)$$

Similarly, by taking $l \to x_2$, the lower limit is given by

$$\lim_{l \to x_2} y_{sc} = \frac{y_2}{2x_2^3}(3x_2 - x_a)x_a^2. \qquad (20)$$

(ii) Curved part passed through the point (x_2, y_2) is given by:

$$y_{cc} = \frac{y_2(3l - x_a)x_a^2}{(3l - x_2)x_2^2}. \quad (0 \le x_a \le x_2 \le l) \qquad (21)$$

In this case, the antenna has curved shape in $0 \le x_a \le x_2$. By partially differentiating eq. 21 with respect to l, we can obtain

$$\frac{\partial}{\partial l}y_{cc} = \frac{3y_2(x_a - x_2)}{(3l - x_2)^2}x_a^2 < 0. \qquad (22)$$

For $0 \le x_a \le x_2 \le l$, $\partial y_{cc}/\partial l$ is always negative. Therefore, y_{cc} is also monotony with respect to l. For the limiting copy, the following upper and lower limits are obtained.

$$\lim_{l \to x_2} y_{cc} = \frac{y_2}{2x_2^3}(3x_2 - x_a)x_a^2, \qquad (23)$$

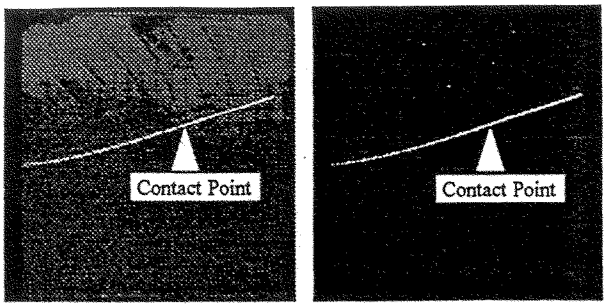

(a) Digitized image (b) Binary image

Figure 5: Captured picture.

$$\lim_{l \to L} y_{cc} = \frac{y_2(3L - x_a)x_a^2}{(3L - x_2)x_2^2}. \quad (24)$$

As expected, the lower limit in Case-(i) is equal to the upper one in Case-(ii). For an arbitrary l ($0 < l \leq L$), the upper and lower limits of the Antenna Shape Function (ASF) are given by

$$\frac{y_2(3L - x_a)x_a^2}{(3L - x_2)x_2^2} \leq \text{ASF} \leq \frac{y_2}{x_2}x_a. \quad (25)$$

Note that the upper and lower limits of ASF form a convex shape as shown in Fig. 3. Now, let us consider a point (x_1, y_1), where $x_1 < x_2$. If (x_1, y_1) is so selected that the point may exist within the convex shape formed by the upper and lower limits, the antenna shape can be uniquely determined. By replacing $x_a = x_1$ and ASF $= y_1$, we can obtain the condition stated in the Theorem.

3.4 Utilization of Two-Points Detecting Method

At first, we extract the points them the antenna from captured picture, and transform from the camera coordinate to the antenna coordinate. Choosing two points sequentially, we check the condition stated in Theorem. If the condition is not satisfied, we choose another two sets of points and check the condition again. If the condition is satisfied, we compute the contact length and contact force by using the analytical solution given in Subsection 3.2. Finally, by averaging all the computed contact lengths and contact forces, we obtain the estimated the contact location and the contact force.

4 Experiments

The image data are got into the computer through a CCD camera with 256×256 dots and 8bits gray scale. For the ease of distinguishing the antenna from the environment, we use a white stainless antenna with a diameter of 0.8mm and a length of 220mm. We believe that one of the big advantages of VBAA is that we can paint the antenna so that it may be easily distinguished from the environment. Figures 5 show captured picture of the antenna and its binary image.

Figures 6 show experimental results of the two points detecting method, where (a) and (b) denote the estimated contact force and the estimated contact distance, respectively. The real lines and circles show the theoretical analysis and the experimental data, respectively. The agreement between analysis and experiments is fairly good. However, we can see some gap between theoretically and experimentally estimated contact distance, especially for relatively large contact distance. This means that the maximum sensing error will be 30mm at the contact distance $l = 20$cm, which corresponds to more than 10% of the contact distance. To cope with this problem, in the following chapter we consider a new compensation method improving the sensing accuracy.

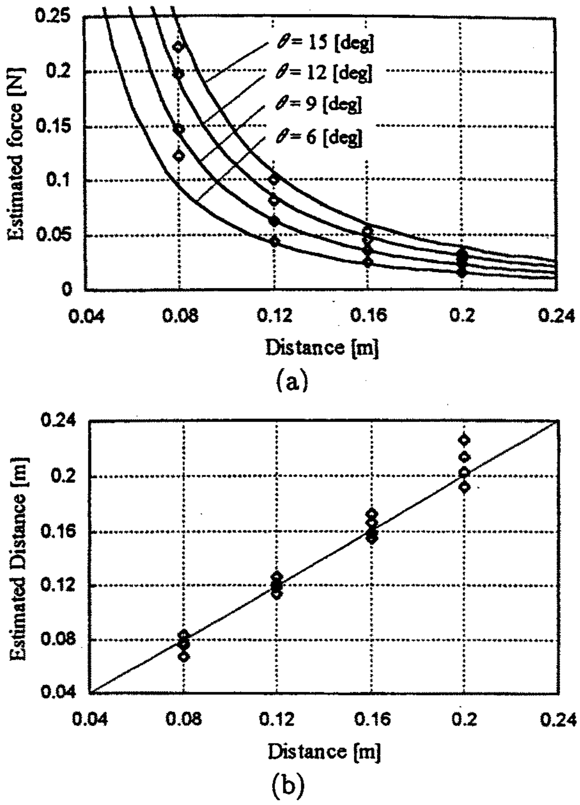

Figure 6: Experimental results without compensation.

5 Discussions

By examining Fig. 6 (b), we found that the estimated contact distances vary according to the pushing angle and the contact distance itself. Based on this consideration, we take the pushing angle into the compensating equation so that we can obtain the estimated contact length and force close to the real ones. The compensation equation is expressed by

$$f' = a_{f0} + (a_{f1} + a_{f2}\theta)\hat{f}, \quad (26)$$
$$l' = a_{l0} + (a_{l1} + a_{l2}\theta)\hat{l}. \quad (27)$$

where l', $\hat{l}$, f' and $\hat{f}$ are the modified contact distance, estimated distance, modified force, and estimated force, respectively. We estimate parameters a_{fi}

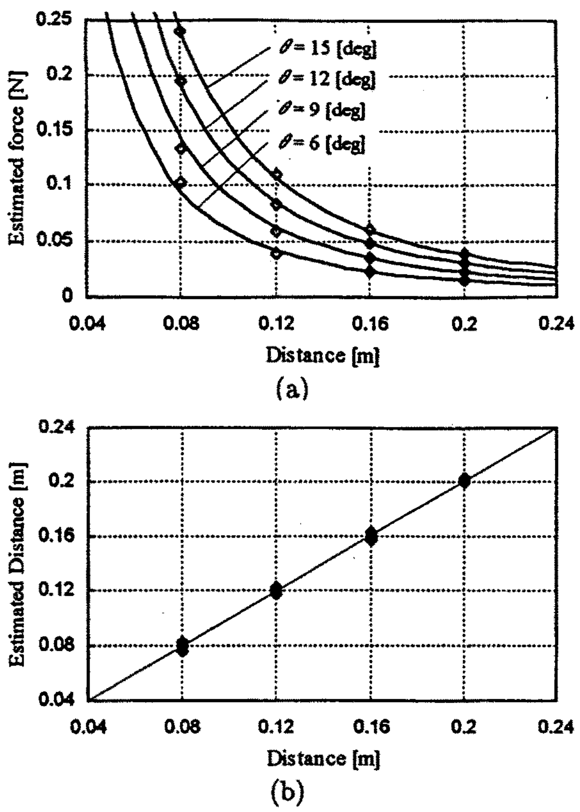

Figure 7: Experimental results with compensation.

and a_{li} $(i = 0, 1, 2)$ in eqs. (26), (27) by using the least square method. Figure 7 shows the improved contact distance and force by using eqs. (26) and (26). It can be seen from Fig. 6 (b) and 7 (b) that the introduction of θ into the compensation equations greatly improves the sensing accuracy. The maximum sensing error is about 3mm over the whole range of the antenna.

6 Conclusions

We discussed the condition of uniquely detecting a contact location and force by using VBAA. The main results obtained in this paper are as follows:
(1) If we can measure two exact points on the antenna, both the contact location and the force can be uniquely computed.
(2) If we cannot measure the exact points on the antenna, uniqueness of solution for the contact location and the force is not always guaranteed. We derived a convenient condition leading to the unique solution.
(3) In order to improve the sensing accuracy, we newly proposed a compensation equation including the pushing angle and showed experimentally that the proposed scheme work effectively.

References

[1] Kaneko, M: Active Antenna, *Proc. of the 1994 IEEE Int. Conf. on Robotics and Automation*, pp2665–2671, 1994.

[2] Kaneko, M., N. Ueno, and T. Tsuji: Active Antenna (Basic Working Principle), *Proc. of the 1994 IEEE Int. Conf. on Intelligent Robotics and Systems*, pp1744–1750, 1994.

[3] Kaneko, M., N. Kanayama, and T. Tsuji: A New Consideration on Active Antenna, *Proc. of the 1995 IEEE/RSJ Int. Conf. on Intelligent Robots and Systems*, pp524–529, 1995.

[4] Kaneko, M., N. Kanayama, and T. Tsuji: 3D Active Antenna for contact sensing, *Proc. of the 1995 IEEE Int. Conf. on Robotics and Automation*, pp1113–1118, 1995.

[5] Kaneko, M., N. Kanayama, and T. Tsuji: Experimental Approach on Artificial Active Antenna, *Fourth Int. Symp. on Experimental Robotics*, pp141–146, 1955.

[6] Ueno, N., M. Kaneko: Dynamic Active Antenna — A principle of Dynamic Sensing, *Proc. of the 1994 IEEE Int. Conf. on Robotics and Automation*, pp1784–1790, 1994.

[7] Ueno, N., M. Kaneko: On A New Contact Sensing Strategy for Dynamic Active Antenna, *Proc. of the 1995 IEEE Int. Conf. on Robotics and Automation*, pp1120–1125, 1995.

[8] Kaneko, M., N. Kanayama, and T. Tsuji: Vision Based Active Antenna, *1996 IEEE Int. Conf. on Robotics and Automation* (to appear).

[9] Russell, R. A.: Closing the sensor-computer-robot control loop, *Robotics Age*, April, pp15–20, 1984.

[10] Wang, S. S. M., and P. M. Will: Sensors for computer controlled mechanical assembly, *The Industrial Robot*, March, pp9–18, 1978.

[11] McKerrow, P.: Introduction to Robotics, *Addison-Wesley*, 1990.

[12] Brooks, R. A.: A robot that walks; Emergent behaviors from a carefully evolved network, *Neural Computation*, vol.1, pp253–262, 1989.

[13] Hirose, S., et.al.: Titan III: A quadrupled walking vehicle, *Proc. of the Second Int. Symp. on Robotics Research*, MIT Press, Cambridge, Massachusetts, 1985.

[14] Schiebel, E. N., H. R. Busby, K. J. Waldron: Design of a mechanical proximity sensor, *Robotica*, vol.4, pp221–227, 1986.

[15] Stansfield, S. A: A robot perceptual system utilizing passive vision and active touch, *The International Journal of Robotics Research*, vol.7, no.6, pp138–161, 1988.

[16] Allen, P. K.: Integrating vision and touch for objects recognition tasks, *The International Journal of Robotics Research*, vol.7, no.6, pp15–33, 1988.